

DOE Award No.: DE-FE0009897

# Quarterly Research Performance Pro- gress Report (Period Ending 12/31/2016)

## Hydrate-Bearing Clayey Sediments: Morphology, Physical Properties, Production and Engineering/Geological Implications

Project Period (10/1/2012 to 9/30/2017)

Submitted by:  
J. Carlos Santamarina



---

Signature

Georgia Institute of Technology  
DUNS #: 097394084  
505 10<sup>th</sup> Street  
Atlanta, GA 30332  
Email: jcs@gatech.edu  
Phone number: (404) 894-7605

Prepared for:  
United States Department of Energy  
National Energy Technology Laboratory

Submission Date: 01/30/2017



U.S. DEPARTMENT OF  
**ENERGY**

**NATIONAL ENERGY  
TECHNOLOGY LABORATORY**

Office of Fossil Energy

**DISCLAIMER:**

This report was prepared as an account of work sponsored by an agency of the United States Government. Neither the United States Government nor any agency thereof, nor any of their employees, makes any warranty, express or implied, or assumes any legal liability or responsibility for the accuracy, completeness, or usefulness of any information, apparatus, product, or process disclosed, or represents that its use would not infringe privately owned rights. Reference herein to any specific commercial product, process, or service by trade name, trademark, manufacturer, or otherwise does not necessarily constitute or imply its endorsement, recommendation, or favoring by the United States Government or any agency thereof. The views and opinions of authors expressed herein do not necessarily state or reflect those of the United States Government or any agency thereof.

## ACCOMPLISHMENTS

**Context – Goals.** *Fine grained sediments host more than 90% of the global gas hydrate accumulations. Yet, hydrate formation in clayey sediments is least understood and characterized. This research focuses on hydrate bearing clayey sediments. The goals of this research are (1) to gain a fundamental understanding of hydrate formation and ensuing morphology, (2) to develop laboratory techniques to emulate “natural” formations, (3) to assess and develop analytical tools to predict physical properties, (4) to evaluate engineering and geological implications, and (5) to advance gas production alternatives to recover methane from these sediments.*

### Accomplished

The main accomplishments for this period include:

- Stiffness characterization of THF hydrate-bearing clay
  - X-ray CT scanning and wave measurements
- Strength of hydrate-bearing fine-grained sediments
  - Frictional contact between hydrate crystals and sediments
  - Non-slip contact between hydrate crystals and sediments
- Gas production: flow patterns in the field

### Plan - Next reporting period

1. Elastic moduli (stiffness) of THF hydrate bearing clays.
2. Prediction of fundamental properties of hydrate-bearing clays
3. Theoretical and analytical study of gas production, including sediment-well interaction during depressurization

## RESEARCH IN PROGRESS

### Stiffness characterization of THF hydrate-bearing clay

X-ray of THF hydrate-bearing kaolinite. Kaolinite is mixed with by mass of 67% of stoichiometric THF solution (i.e.,  $H_2O:THF = 81:19$ ) and packed within a self-loaded consolidation cell for wave measurement. Hydrate formation is triggered by cooling. Figure 1 shows the obtained CT images after hydrate formation. THF hydrates are segregated as lenses and nodules from the matrix clay soils. Hydrate saturation  $S_h$  in this case is defined as the volume of hydrate over the total specimen volume, rather than the volume of hydrate over the volume of voids for sandy specimens. The shown specimen has a hydrate saturation  $S_h = \sim 15\%$ .

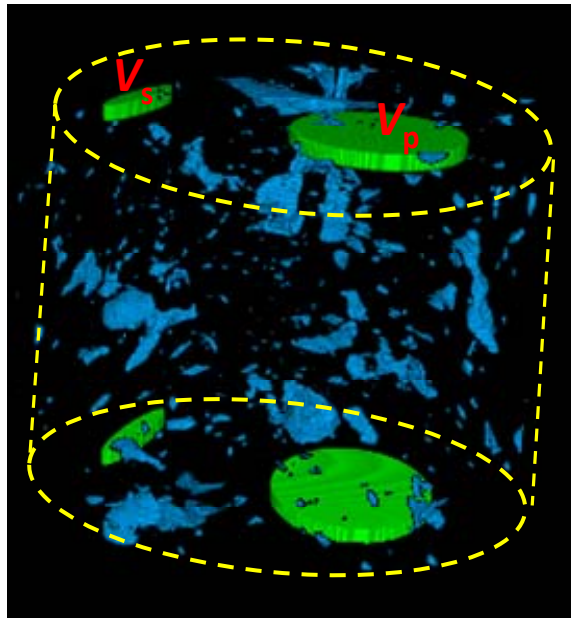


**Figure 1:** 3D CT image of THF hydrate-bearing kaolinite. Segregation hydrates (blue) are formed within kaolinite specimen (made transparent). The pairs of bender elements (for S-wave measurement) and piezopad (for P-wave measurement) are also shown in the image. Specimen diameter is about 1 inch.

Both P- and S-waves are measured during hydrate formation, loading, unloading, and hydrate dissociation. By doing so, all elastic moduli (Young's, shear, bulk, and constrained moduli) and Poisson's ratio can be obtained. Figure 2 shows the obtained wave signatures for the above specimen at different stages of the experiments.

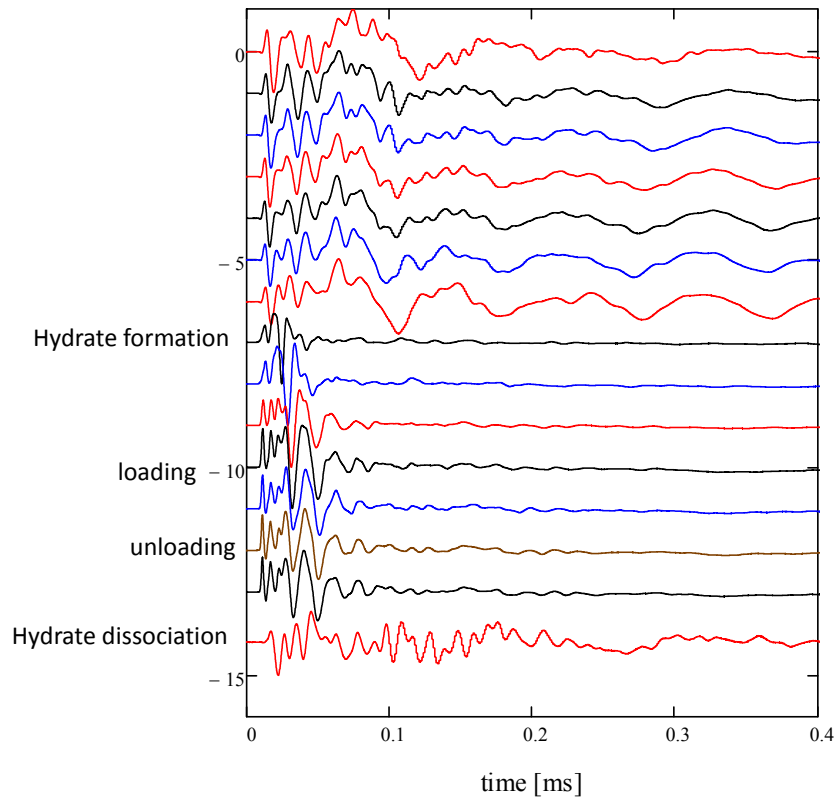
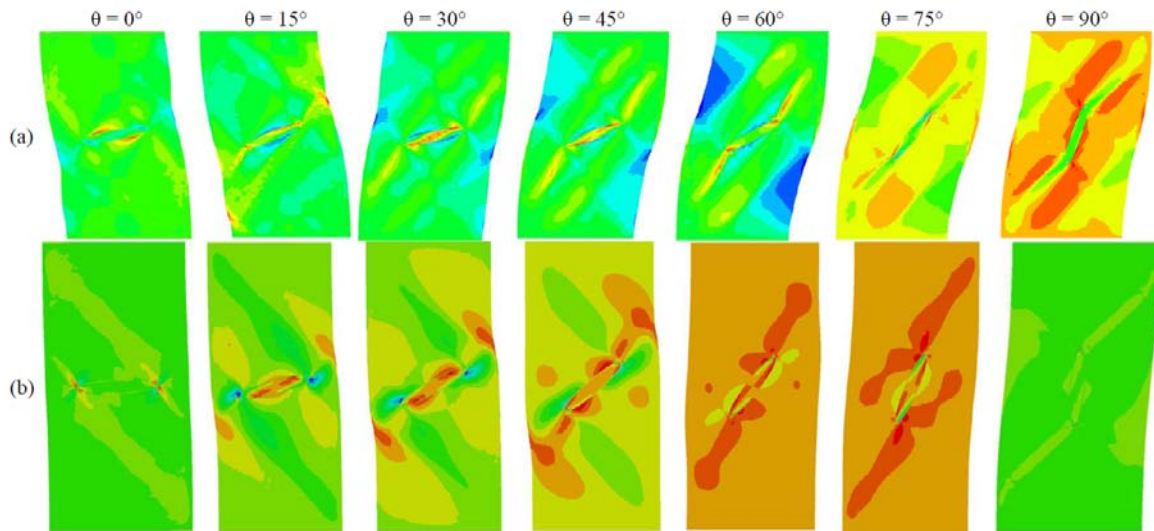


**Figure 2:** Measured p- and s- wave signatures in THF hydrate-bearing kaolinite during hydrate formation, loading, unloading, and hydrate dissociation processes.

### Strength of hydrate-bearing fine-grained sediments

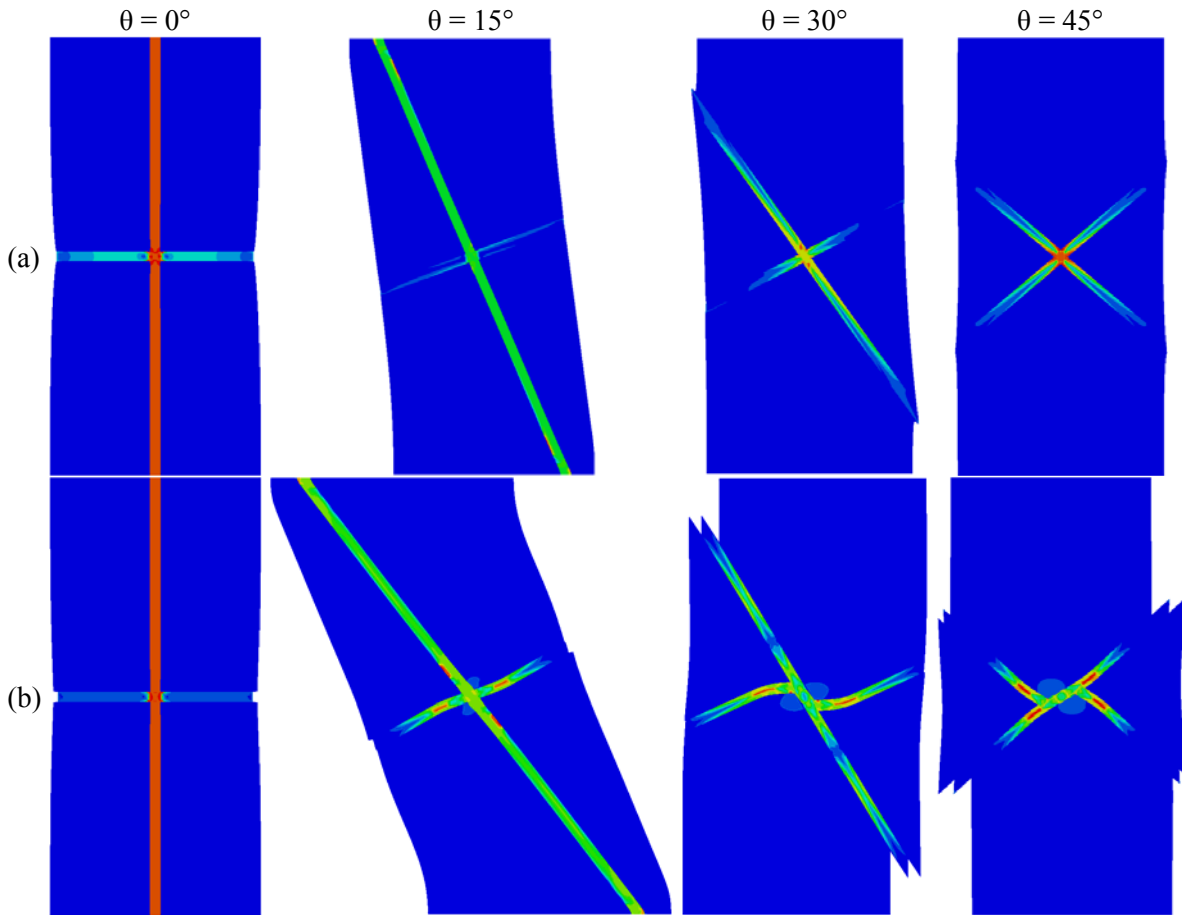
The strength analyses in this section consist of two cases, frictional and non-slip hydrate-sediment interfaces. The hydrate lens elements share the same nodes with the soil elements in non-slip contact simulations. This corresponds to when the hydrate is in growing or is stable. Interfaces between the hydrates and the sediments are rough and jagged. Therefore, there is unlikely to be slippage between the hydrates and sediment in the loading process. However, when the hydrate dissociates during gas production, the dissociation firstly occurs on the interface. Consequently, the contact between hydrates and sediments becomes slippery due to the presence of produced gasses. The characterization of the strength of the sediments then uses frictional contacts. The simulation uses a thin layer of material with a low friction angle ( $\varphi = 5^\circ$ ) to represent the frictional contact.

Figure 3 presents the displacement and in-plane shear stress field of the hydrate-bearing fine-grained sediments. The localized in-plane shear stress induces the later development of shear bands. When the interface is non-slip, the hydrate mass enhances the sediment strength by the inhibition of shear band formation. Therefore, two shear bands form around but do not cross the hydrate lens. However, when there is a frictional interface, one shear band develops along the interface. The shear band forms at a much lower vertical strain level in frictional conditions compared to the non-slip case.



**Figure 3:** Fine-grained sediment with a single segregated hydrate lens subjected to shear. In-plane shear stress fields for various lens orientation  $\theta$ . (a) Frictional hydrate-sediment interface, (b) Non-slip hydrate-sediment interface.

Figure 4 shows the simulation results of sediments that contain cross hydrate lenses. The hydrate lenses behave as reinforcements to the sediment. When the load transfers directly through the hydrate lenses ( $0^\circ$ ), the overall sediment strength reaches its peak. The influence of the interface strength is negligible in this condition. However, a slight tilt of the hydrate lenses can result in a significant strength decrease. The shear resistance of the overall sediment controls the load capacity, and the interface strength becomes critical as the angle of orientation  $\theta$  increases. Shear stress localizes at the intersection of hydrate lenses in the slip interface condition. The hydrate yields and breaks when the shear force exceeds its strength. This could be an important failure mechanism when gas hydrate dissociates.



**Figure 4:** Fine-grained sediment with two normally-intersecting hydrate lenses at different orientation  $\theta$ . Von-Mises-stress =  $([(\sigma_1 - \sigma_2)^2 + (\sigma_1 - \sigma_3)^2 + (\sigma_3 - \sigma_2)^2] / 6)^{1/2}$  fields. (a) Frictional hydrate-sediment interface, (b) Non-slip hydrate-sediment interface.

## Gas production: flow patterns in the fields

Different hydrate deposits have different in situ temperature, pressure, effective stress, pore pressure, and sediments characteristics (See Dai et al., 2012 JGR and Lei, PhD thesis – Georgia Tech, 2016). Figure 5 illustrates the field data plotted in terms of vertical effective stress normalized by characteristic capillarity ( $\sigma'/C_{gw}^*$ ) and phase pressure difference normalized by characteristic capillarity ( $(P_g - u_w)/C_{gw}^*$ ) as well. We assume the characteristic pore throat is 1/10 of D10 and plot the pressure difference between the gas and water of 1 MPa or 3 MPa. Analyses show that gas does not flow when the water pressure is 3 MPa lower than the gas pressure at a number of sites that include Blake Ridge. Gas flow through pores usually occurs in coarse-grained sediments. Shallow marine sediments in conditions where effective stress is low favor gas flow through gas driven fractures. The pressure difference between the gas and water could be generated through gas pressure increases by thermal stimulation or through decreases in water pressure. Note that the gas pressure in the sediment cannot be larger than the pressure on the hydrate phase boundary during continuous gas production.

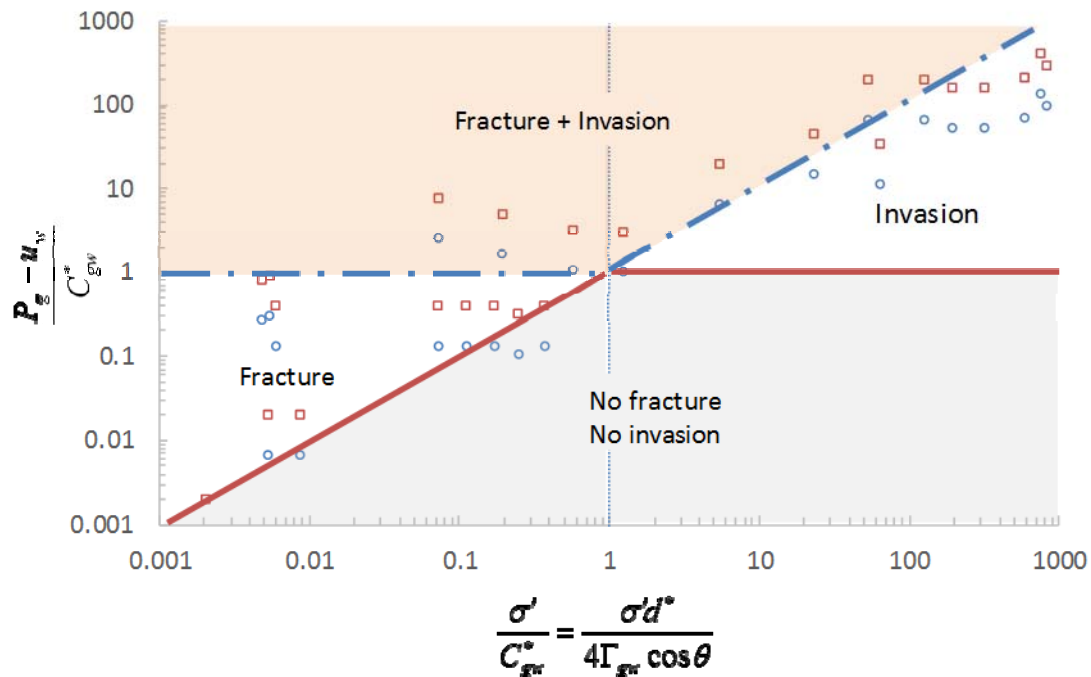


**Figure 5.** Balance between the effective stress  $\sigma'$ , characteristic capillary pressure  $C_{gw}^*$  and the pressure difference between the gas and water  $P_g - u_w$ . Different regions inferred from equilibrium conditions. Dots represent different hydrate reservoirs. We assume the pressure difference for all the sites is either 1MPa ( $\circ$ ) or 3MPa ( $\square$ ).



## MILESTONE LOG

Milestone	Planned completion date	Actual completion date	Verification method	Comments
Literature review	5/2013	5/2013	Report	
Preliminary laboratory protocol	8/2013	8/2013	Report (with preliminary validation data)	
Cells for Micro-CT	8/2013	8/2013	Report (with first images)	
Compilation of CT images: segregated hydrate in clayey sediments	8/2014	8/2014	Report (with images)	
Preliminary experimental studies on gas production	12/2014	12/2014	Report (with images)	
Analytical/numerical study of 2-media physical properties	5/2015	5/2015	Report (with analytical and numerical data)	Additional studies in progress
Experimental studies on gas production	12/2015	12/2015	Report (with data)	Additional studies in progress
Early numerical results related to gas production	5/2016	2/2016	Report	Additional studies in progress
Comprehensive results (includes Implications)	9/2016	9/2016	Comprehensive Report	

## PRODUCTS

- **Publications & Presentations:**

Jang, J., Sun, Z. and Santamarina, J.C., (2017) Capillary pressure across a pore throat in the presence of surfactants. *Water Resources Research*. (Accepted)

Jang, J. and Santamarina, J.C., (2016). Hydrate bearing clayey sediments: Formation and gas production concepts. *Marine and Petroleum Geology*, 77, pp.235-246.

Shin, H. and Santamarina, J.C., (2016). Sediment–well interaction during depressurization. *Acta Geotechnica*, pp.1-13.

Dai, S., Shin, H. and Santamarina, J.C., (2016). Formation and development of salt crusts on soil surfaces. *Acta Geotechnica*, 11(5), pp.1103-1109.

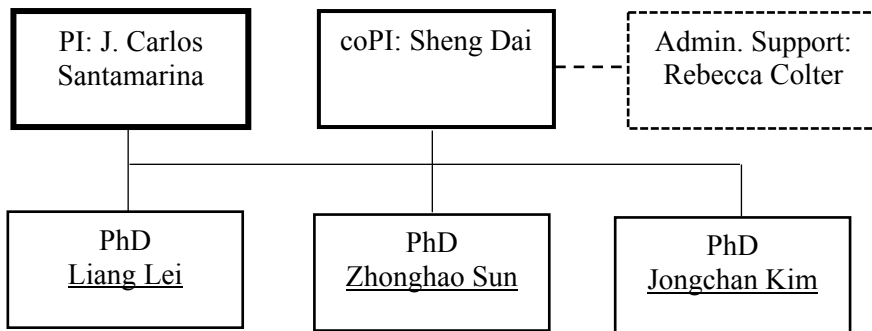
- **Website:** Publications and key presentations are included in <http://pmrl.ce.gatech.edu/> (for academic purposes only)
- **Technologies or techniques:** X-ray tomographer and X-ray transparent pressure vessel
- **Inventions, patent applications, and/or licenses:** None at this point.
- **Other products:** None at this point.

## **PARTICIPANTS & OTHER COLLABORATING ORGANIZATIONS**

*Research Team:* The current team involves:

- Liang Lei (PhD student)
- Zhonghao Sun (PhD student)
- Jongchan Kim (PhD student)
- Sheng Dai (Assistant Professor)
- Carlos Santamarina (Professor)

*Research Team:*



### **IMPACT**

Understanding of fine grained hydrate-bearing sediments.

### **CHANGES/PROBLEMS:**

None at this point.

### **SPECIAL REPORTING REQUIREMENTS:**

We are progressing towards all goals for this project.

### **BUDGETARY INFORMATION:**

As of the end of this research period, expenditures are summarized in the following table.

Baseline Reporting Quarter DE-FE009897	Budget Period 4			Budget Period 5			
	Q3		Q4		Q1		Q2
	Q3	Cumulative Total	Q4	Cumulative Total	Q1	Cumulative Total	1/1/17 - 3/31/17
<b>Baseline Cost Plan</b>							
Federal Share	41,547	585,846	41,547	627,393	0	627,393	627,393
Non-Federal Share	11,935	170,839	11,935	182,774	0	182,774	182,774
Total Planned	53,482	756,685	53,482	810,167	0	810,167	810,167
<b>Actual Incurred Cost</b>							
Federal Share	45,285	539,627	17,607	557,234	11,416	568,650	
Non-Federal Share	5,056	167,612	2,505	170,116	5,009	175,126	
Total Incurred Costs	50,341	707,238	20,112	727,350	16,425	743,775	
<b>Variance</b>							
Federal Share	3,738	-46,219	-23,940	-70,159	11,416	-58,743	
Non-Federal Share	-6,879	-3,227	-9,430	-12,658	5,009	-7,648	
Total Variance	-3,141	-49,447	-33,371	-82,817	16,425	-66,392	

## National Energy Technology Laboratory

626 Cochrans Mill Road  
P.O. Box 10940  
Pittsburgh, PA 15236-0940

3610 Collins Ferry Road  
P.O. Box 880  
Morgantown, WV 26507-0880

13131 Dairy Ashford Road, Suite 225  
Sugar Land, TX 77478

1450 Queen Avenue SW  
Albany, OR 97321-2198

Arctic Energy Office  
420 L Street, Suite 305  
Anchorage, AK 99501

Visit the NETL website at:  
[www.netl.doe.gov](http://www.netl.doe.gov)

Customer Service Line:  
1-800-553-7681



U.S. DEPARTMENT OF  
**ENERGY**

**NATIONAL ENERGY  
TECHNOLOGY LABORATORY**